

# Simulating isothermal crystallisation during phase separation of oxide glasses and the percolation behaviour of these glass-ceramics

I. SINHA

*MTP Division, National Metallurgical Laboratory, Jamshedpur 831007, India*  
E-mail: jitsinha@yahoo.co.in

R. K. MANDAL

*Department of Metallurgical Engineering, Banaras Hindu University, Varanasi 221005, India*  
E-mail: rkmandal@satyam.net.in

---

We modelled the isothermal crystallisation of oxide glasses during their phase separation using the static Monte Carlo technique as in the site percolation model. Initial compositions such that crystallisation can only occur in the evolving glassy matrix phase were considered. The isothermal crystallisation behaviour in terms of model analogues of crystal nucleation and growth were found to qualitatively correspond to the experimental results. The percolation behaviour of the crystalline phase in the evolving glass-ceramic was then studied. The validity of the scaling assumption for percolation phase transition was first tested for the considered systems and then various critical exponents at and near the percolation threshold was estimated. It was found that scaling hypothesis followed for all cases considered in the present investigation. © 2002 Kluwer Academic Publishers

---

## 1. Introduction

The process of phase separation of oxide glasses and their crystallisation can either occur at two different temperatures or they may be occurring concurrently at the same temperature depending on the choice of experimental conditions. In the former case, the microstructures of oxide glasses resulting from glass-in-glass phase separation primarily control the microstructural evolution of glass-ceramics [1, 2]. However, for the latter case the compositional changes in the glass occur along with crystallisation [1]. It is imperative to understand how and to what extent different changes taking place in the system affect microstructural modifications during the crystallisation of glasses. Further, an important aspect of this problem is the effect on connectivity of the clusters of the crystalline phase near its percolation threshold in the resulting glass-ceramics [3, 4]. Keeping these in view, we use the classical site percolation model [5] for the simulation of isothermal crystallisation (IC) of oxide glasses. In the present paper, we only deal with simultaneous phase separation and crystallisation. We will present the results for crystallisation of prior phase-separated glasses elsewhere. Further, we only consider phase separation by nucleation. For this, we first qualitatively model and present the results (in Section 2) of the isothermal crystallisation in glasses undergoing phase separation using the classical site percolation model. Next, we study different aspects of cluster statistics of the crystalline phase at or near its percolation threshold in Section 3.

## 2. Simultaneous phase separation and crystallisation of oxide glasses

We start with a model system (called system 1 and constructed using the static Monte Carlo technique) with isothermal crystallisation kinetics, which qualitatively resembles a homogeneous oxide glass. The salient features of this system pertain to homogeneous nucleation and polymorphic crystallisation. The system is comprised of sites. The sites are assigned values between 0 and 1. The distribution of these values in the interval 0 to 1 is Gaussian. The spatial distribution of numbers assigned to sites around each site, in the present study, is also near to a Gaussian. This is usually achieved by adopting an averaging procedure with its inclusion of nearest, second and third nearest neighbours of a chosen site. A site value when compared with the crystallisation probability of the system ( $p$ ) gives the site crystallisation probability. That is, if the site value is less than or equal to  $p$  then the site is identified as crystalline one. The initial value of  $p$  is 0 and then is incremented in steps of 0.001. Since crystallisation occurs in units of a site, therefore we assume the crystallisation of an isolated site surrounded by glassy matrix a nucleation event. Two sites are defined as neighbours if they are nearest or second nearest or third nearest neighbours. As  $p$  is incremented the growth of these nuclei occurs by crystallisation of their neighbouring sites. Such crystalline clusters are known as grains. At some value of  $p$ , these grains may impinge at a grain boundary. Thus, number of grains present also gives the number

of crystal nuclei in the system. We assume from experimental observations that increase in heat treatment time is the analogue of increase in  $p$ . However, the values assigned to sites according to system 1 spatial distribution remain the same throughout this process. Thus, in this model the crystal nucleation and growth behaviour of the systems depend only on the overall and spatial distribution of values assigned to sites in the system. The latter, will of course, be a function of temperature, which cannot be handled, in the present model. This therefore implies a single stage crystallisation process unlike those followed in controlled crystallisation of glasses. We shall refer to the foregoing, the progress of crystallisation with increase in  $p$ , as the isothermal crystallisation algorithm (ICA). To understand how this model may be used here, in the next section, we present a physical picture of the process of simultaneous phase separation and crystallisation based on experimental observations in the following sub-section.

### 2.1. The physical picture

Phase separation of oxide glasses gives rise to two glassy phases. One is network forming oxide rich (NFR) and the other network forming oxide lean (NFL) composition. The latter, owing to its composition, has a greater tendency to crystallize than the initial glass. Crystal nucleation occurs within this glassy phase and is determined by its composition [1]. A typical temperature-composition diagram of a binary glass-system that undergoes phase separation is shown in Fig. 1. We consider a system in which composition  $c_a$  is NFR and composition  $c_b$  is NFL and that, at the given temperature, crystallisation can only occur in the phase with composition  $c_b$ . We only study phase separation and crystallisation of glasses of composition in region III. Here phase separation takes place by formation of droplets of composition  $c_a$  through nucleation in the resulting  $c_b$  matrix. The most recent studies in this composition regime are on BaO-SiO<sub>2</sub> [1, 6, 7] and

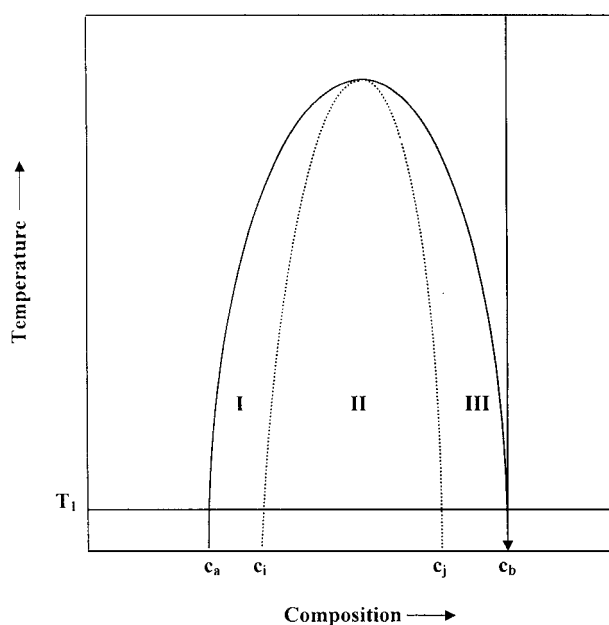


Figure 1 Schematic of a typical temperature-composition diagram of glass systems: the arrow pointing towards composition  $c_b$  is assumed to be that of system 1.

Li<sub>2</sub>O-SiO<sub>2</sub> systems [1, 8]. As phase separation progresses with time, more and more droplets of  $c_a$  phase are formed and the composition of the matrix tends towards  $c_b$ . This also means that matrix composition displays variation. As the matrix becomes more  $c_b$  rich, the crystal nucleation rate increases. Initially, a curved plot of number of crystals per unit volume against time is observed for such cases [1]. The crystal nucleation rate approaches a constant value at longer times as the matrix phase reaches its equilibrium composition  $c_b$ . The constant nucleation rates approached at later stage are found to be same because the eventual composition ( $c_b$ ) of the matrix phase is identical for all these glasses [1]. As the initial glass composition is shifted away from  $c_b$ , the time required to achieve constant nucleation rate (induction time) is found to decrease.

### 2.2. The model

Experimental observations are available only on the effect of phase separation on crystal nucleation and not on the crystal growth or the overall crystallisation kinetics [1, 6, 7]. We try to utilise this information to simulate the overall (isothermal) crystallisation process of a glass undergoing phase separation (with initial composition in region III in Fig. 1). As mentioned above crystallisation can occur only in the evolving matrix phase since  $c_b$  is the NFL composition. In literature it is mentioned that the changing composition of the matrix phase in such a system affects the crystallisation. However, the nature of this change has not been clarified. In our model we make the assumption that as phase separation progresses with time, more and more droplets of  $c_a$  phase are formed and the fraction of matrix with composition  $c_b$  accordingly increases. Thus, droplets always form with composition  $c_a$  whereas those regions of matrix, which are prone to crystallisation, attain composition  $c_b$ . Thus, while crystallisation occurs with increase in the value of  $p$ , we need to take into account the effect of changing composition through variation in spatial site value distributions. However, this would make the algorithm complex and computationally intensive. In addition, the initial configuration of the system will change with  $p$  thus making the study of percolation characteristics of the system difficult. Therefore, instead of trying to follow the temporal evolution, we prepare the model system such that the different states that will be encountered during phase separation are present in it. For achieving this, we proceed as follows.

We consider a three-dimensional (3D) cubic array of  $L \times L \times L$  sites (where  $L = 150$  for IC studies). Two initial glass compositions, such that they eventually result in 0.1 and 0.2 fraction of droplet phase in the glass, are chosen. The systems corresponding to these are labelled 2a and 2b respectively. The algorithm of the model is implemented in the following manner (see flow chart in Fig. 2).

We begin by considering an array  $A$  having site values according to system 1 distribution. This distribution is assumed to represent the crystallisation behaviour of the homogeneous glass of composition  $c_b$ . To create a droplet in the model system we randomly chose a site in array  $A$ . If the average of the value of the site and its

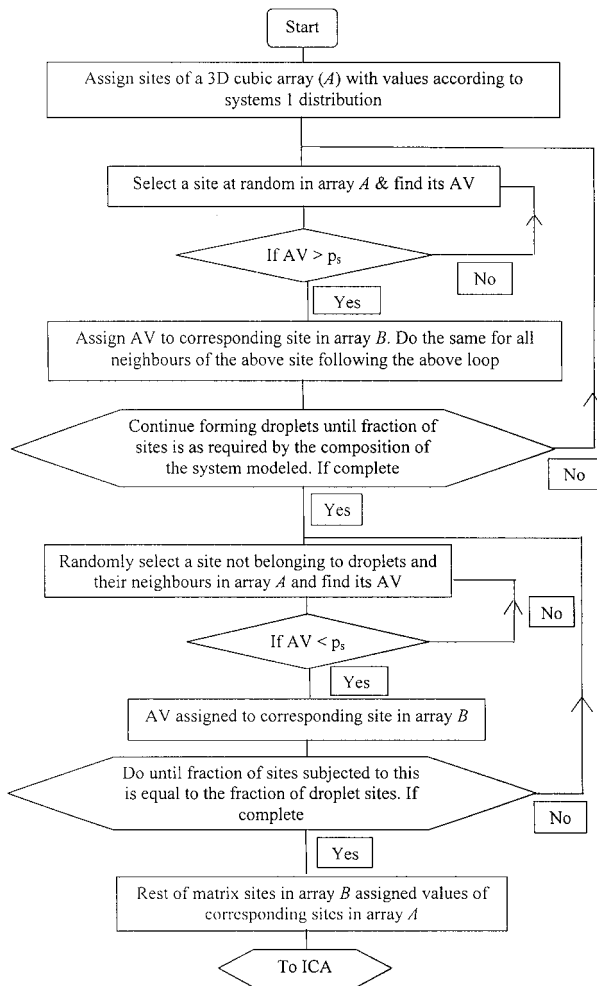


Figure 2 Flowchart for implementation of the algorithm for modelling simultaneous phase separation and crystallisation.

neighbours (called the AV henceforth) is higher than a certain threshold value (called the  $p_s$  value) then it is counted as part of a new droplet and AV is assigned to this site in a new array (called  $B$ ). The nearest, second nearest and the third nearest neighbours are defined as neighbours of a site. Rest of the sites comprising the droplet are found and assigned values (in array  $B$ ) by following the same procedure for the sites neighbouring the initially identified droplet site. To model another droplet we follow the parallel procedure. This is continued to achieve the desired fraction of the droplets viz. 0.1 and 0.2 respectively for system  $2a$  and  $2b$ . The values of  $p_s$  corresponding to these cases are determined a priori by conducting the simulation to attain respective fractions of droplets in array  $B$  from array  $A$ . Having created the desired fraction of droplets, we compare the AV of a given site, not belonging to droplets and its neighbours, with  $p_s$ . If AV is less than  $p_s$ , then this value is assigned to corresponding site in array  $B$ . This is continued through the random selection of sites in array  $A$  and the process is terminated when the fraction of such sites equals to those of droplets in array  $B$ . It is obvious that many of the sites are still without consideration in old array  $A$ . They are correspondingly transformed to array  $B$  with the old system 1 distribution. Therefore, the matrix sites in array  $B$  have values according to two Gaussian distributions. One belonging to system 1 and other corresponds to the above mentioned distribution

(henceforth called second distribution). The probability of crystallisation of a fraction of second distribution sites is less than those sites having system 1 values. Owing to this, the system may demonstrate an initially slow crystal nucleation rate that will increase gradually to the steady state rate of system 1. Thus, the fraction of sites in the system assigned values according to second distribution represents the changing composition of the matrix and is hence taken as 0.1 and 0.2 respectively of the total sites in the systems  $2a$  and  $2b$  respectively. The next question is how the sites belonging to second distribution should be spatially distributed in the matrix.

During phase separation, the composition change in different regions of the matrix may not be uniform [10]. When a droplet is formed composition in its immediate neighbourhood changes first and consequently crystal nucleation may be more probably in the neighbourhood of droplets. To model these compositional changes in the matrix in terms of site crystallisation probabilities, sites that are nearest neighbours to a droplet are not subjected to the second distribution. They have the values initially assigned to them according to the system 1 distribution. This is to ensure that crystallisation in the immediate neighbourhood of droplets is more probable. Rest of the sites conforming to either of the two distributions may be distributed randomly in the matrix.

These systems are now subjected to the isothermal crystallisation algorithm (ICA) as mentioned earlier. The ICA is terminated as soon as the fraction of crystalline sites in systems  $2a$  and  $2b$  equals the NFL phase fraction (or as soon as  $p > p_s$ ). In the next two subsections, results in terms of numbers of crystal nuclei and average grain size are presented and discussed.

### 2.3. Results and discussion

The nucleation behaviour for system  $2a$  and  $2b$  are observed in terms of number of crystal nuclei per site ( $n_1$ ). This is found by dividing the number of grains present at a  $p$  with the total number of sites in the system. By studying the variation of average grain size ( $a_{gs}$ —calculated by dividing the number of crystalline sites by the number of grains in the system) in the system with increase in  $p$ , we monitor growth rates. For the sake of comparison, we also present crystal nucleation and growth curves of homogeneous glass (system 1) in terms of  $n_1$  and  $a_{gs}$ . All plots given here are line plots. This is owing to the high density of data points. For all  $n_1$  and  $a_{gs}$  plots, the average values of the standard deviation of the data points in each plot over the range of  $p$  values where the respective quantities increase at a constant rate is always below 0.5%.

Fig. 3a shows  $n_1$  versus  $p$  for systems 1,  $2a$ , and  $2b$  respectively. The general characteristics of curves  $2a$  and  $2b$  are similar to that of 1. In the initial stages,  $n_1$  shows a non-linear increase. This models the effect of changing composition during phase separation on crystallisation. During this period, only small regions (near the droplets) have the composition  $c_b$ . Since the fraction of sites in the matrix where crystallisation is probable is small, hence crystal nucleation rates are slower. After the initial non-linear increase, the three curves

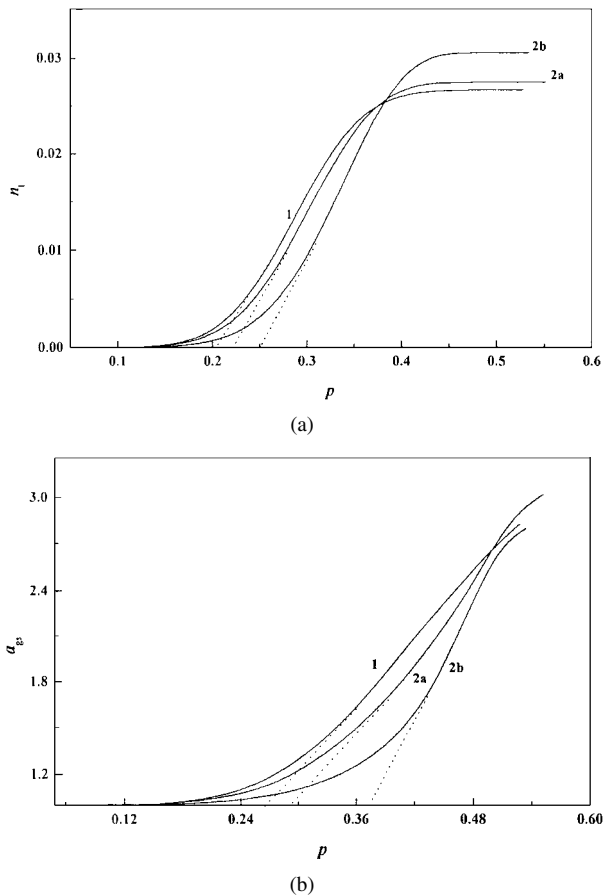


Figure 3 (a) Variation of  $n_1$  for systems 1, 2a and 2b with  $p$ . (b) Depicts the nature of variation of  $a_{gs}$  in systems 1, 2a and 2b with  $p$ .

increase at almost same constant rates. This models the effect of the achievement of the composition  $c_b$  (in all three systems), on completion of phase separation, over the rest of the matrix sites where crystallisation has not yet occurred. Further, the induction period of this, increase with decrease in fraction of the matrix (NFL) phase in the system. This is because the period required for achieving the completion of phase separation (and constant composition of the matrix phase) increases.  $n_1$  decreases with increasing  $p$  at later stages and finally reaches a constant value. The total number of nuclei eventually formed increases with increasing fraction of the matrix phase. Hence, all the features of experimental observations of crystal nucleation during phase separation [1, 6, 7] have been incorporated qualitatively in our model. It is important to mention here that the attainment of the above in the present model is owing to the consideration of two types of Gaussian distribution (mentioned in the preceding subsection) invoked for understanding the crystallisation behaviour of the matrix phase in systems 2a and 2b. Increase in fraction of sites that have lesser probability of crystallisation than sites belonging to system 1 distribution models the composition change.

$a_{gs}$  versus  $p$  plots for these systems are given in Fig. 3b. The induction period for growth of system 1 is not very different from its induction period for nucleation but this is not so for systems 2a and 2b. For these two systems, the induction periods for nucleation and growth differ by more than 0.1 (in units of  $p$ ). Sites having values belonging to second distribution may be

neighbours of those belonging to system 1 distribution. The crystal growth rate thus increases slowly (compared to the initial rate of increase of number of crystal nuclei) in the initial stages of crystallisation. This resembles the situation where region has attained the  $c_b$  (cf. Fig. 1) but its neighbourhood has not. Owing to this, different induction periods for crystal nucleation and growth (Fig. 3a and b) are observed. Hence, this is also an effect of gradual achievement of a uniform matrix composition on crystallisation. After, the initial non-linear portions,  $a_{gs}$  increase with constant rates. This signifies that composition  $c_b$  has been attained in the rest of the matrix. In later stages of the transformation, this rate decreases with increase in  $p$  and this decrease is more significant for systems 2a and 2b.

The difference in the total number of crystal nuclei formed (on completion of crystallisation process) in system 1, 2a and 2b is again due to impeded growth. Sites not available for crystal nucleation due to growth (ingestion) in system 1 are also possible nucleation sites in systems 2a and more so in 2b. This increases the total number of crystal nuclei formed in the system. However, there are no experimental observations of this nature. Rarely crystallisation treatments are carried out to completion [10].

### 3. Percolation characteristics

The properties of the resulting glass-ceramics are sensitive to the nature of connectivity of the ceramic phase in the glassy matrix [4]. Hence understanding various parameters pertaining to connectivity assumes special significance for such systems. In this section, we try to understand how phase separation during crystallisation affects the connectivity of the crystalline phase from percolation characteristics of the systems 2a and 2b.

The behaviour of the systems at or near percolation threshold, according to the scaling theory of percolation phase transition, is given by different characteristics of cluster size and its distribution [5, 11]. The various terms describing these characteristics are expressed in terms of increase in fraction of crystalline phase ( $x$ ) in the system. This ( $x$ ) is interpreted as the probability of any site in the system being crystalline. The fraction of crystalline phase at which percolation is first observed is the percolation threshold ( $x_c$ ). A critical exponent describes each of these characteristics at or near  $x_c$ . The critical exponents we find here are  $\tau$ ,  $\beta$  and  $\gamma$ . The fundamentals and other details relating to these are summarised in the book by Stauffer and Aharony [5]. We reproduce some of the relevant expressions for the sake of continuity. The scaling hypothesis stipulates the form of the scaling function as

$$n_s(x)/n_s(x_c) = v_s(x) = \exp(-z) = f(z) \quad (1)$$

where  $z \propto (x - x_c)s^\sigma$ ,  $n_s$  is the number of clusters with cluster size  $s$  (= number of sites in a cluster) and  $\sigma$  is a critical exponent. To test whether this scaling assumption is valid for a system we plot  $n_s(x)/n_s(x_c)$  versus  $z$  for different  $s$  values. The value  $z$  for different cluster sizes  $s$  is calculated using the best numerical estimate for the universal value of  $\sigma = 0.45$  for 3D systems

based on report in literature [5]. The form of this function should not change for different cluster sizes. Since scaling theory is not applicable to clusters of small size [5], therefore we only consider two intermediate cluster size ranges. The first size range includes all clusters with sizes ranging from 64 to 127 and the second includes clusters that can have any size from 128 to 255.  $s$  is the geometric mean of the two border sizes.

At the percolation threshold  $x = x_c$ , we have scaling relation

$$n_s(x_c) \propto s^{-\tau} \quad (2)$$

where exponent  $\tau$  defines the number  $n_s(x_c)$  of  $s$  cluster only at  $x = x_c$ . Thus,  $\tau$  is given by the slope of  $n_s$  versus  $s$  plots. This excludes the infinite cluster.

Another important exponent  $\beta$  describes the variation of the probability of any arbitrary site in the system being a part of the percolation cluster ( $P$ ) as  $x$  increases beyond  $x_c$ .

$$P \propto (x - x_c)^\beta \quad (3)$$

where  $\beta = (\tau - 2)/\sigma$ . The slope of  $\log P$  versus  $\log(x - x_c)$  plot gives  $\beta$ . To implement this we find the number of sites in the infinite cluster above  $x_c$ .

The variation of the mean cluster size  $S = \Sigma n_s s^2 / \Sigma n_s s$  with  $x$  is understood in terms of exponent  $\gamma$  by

$$S \propto |x - x_c|^{-\gamma} \quad (4)$$

where  $\gamma = (3 - \tau)/\sigma$ . The slope of  $\log S$  (where  $S = \Sigma n_s s^2 / \Sigma n_s s$ ) versus  $\log|x - x_c|$  plots give the  $\gamma$  value. We calculate its values both above and below  $x_c$ .

The value of the percolation threshold of a system is unique only for an infinite system. Therefore it is necessary that we first determine an effective percolation threshold  $x_c(L)$  for a finite size system. This is the most probable value of  $x$  for the system at the percolation threshold found from a large number of Monte Carlo (MC) simulations [12]. We used 500 such MC simulations of 3D cubic arrays of size corresponding to  $L = 180$  to find  $x_c(L)$  for each system. To find exponents  $\tau$ ,  $\beta$  and  $\gamma$  we use average values of cluster statistics parameters of 200 MC simulations on 3D systems of size corresponding to  $L = 200$ . Thus we use different system sizes for determination of  $x_c(L)$  and the critical exponents. Smaller system size and more number of MC simulations enables us to accurately estimate the value of  $x_c(L)$  more efficiently. However, for estimation of values of critical exponents  $\tau$ ,  $\beta$  and  $\gamma$  we need

larger system sizes. Critical exponents found from one set of 200 MC simulations vary from the value found from another set by not more than  $\pm 0.005$ . For a finite system, the boundaries of the lattice cut the infinite cluster into several pieces, increasing the number of finite clusters. To reduce this effect the size of a cluster is determined using periodic boundary conditions [5, 13]. Finally, from the estimates of critical exponents of different systems we determine whether their critical behaviour conforms to the universality concept. According to this concept, different systems of same dimensionality have the same value for each critical exponent [5] for infinite or very large systems (which approach the 'thermodynamic limit'). In contrast to this, these exponents for finite systems display deviation from their universal values (finite size effects). In the next section, results in terms of the critical exponents found by using the procedures described above are presented and discussed.

### 3.1. Results and discussion

The values of systems characteristics and critical exponents of systems  $2a$  and  $2b$  are given in Table I. For the sake of comparison, we have also included percolation characteristics of system 1. The  $x_c(L)$  and approximate  $P$  values for each system of the size corresponding to  $L = 180$  is given in the second and third column of Table I respectively. Values of critical exponents  $\tau$ ,  $\beta$  and  $\gamma$  are given in the fourth, fifth, sixth and seventh columns of Table I. The best numerical estimates [5] of the universal value of these critical exponents are also given in the second row of this table.

Figs 4a and b show the  $n_s(x)/n_s(x_c)$  versus  $z$  plots for systems  $2a$  and  $2b$  respectively. Generally, the data points for the two cluster sizes follow the same curve for both systems. Thus, the scaling theory is found to be valid for these two systems. The  $\log n_s$  versus  $\log s$  plots for systems  $2a$  and  $2b$  are shown in Fig. 5. Owing to larger finite size effects, system  $2b$  has a higher slope than system  $2a$  and its data points show slight deviation from linearity at higher values of  $s$ . The deviation from the universal value is around 4% and 6% for system  $2a$  and  $2b$  respectively. The higher  $\tau$  values obtained for systems  $2a$  and  $2b$  tells us that there is relatively lesser number of larger clusters in the system at  $x_c$  compared to system 1. Owing to impeded growth, the required proportion of larger clusters is not formed at percolation. This effect is increased, as expected, when phase separation is increased, by making the initial composition more NFR (system  $2b$ ). The  $x_c$  and  $P$  value also show increase with increase in phase separation.

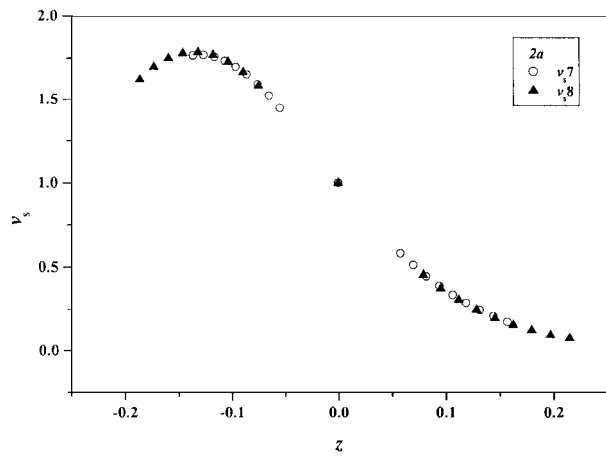
TABLE I System characteristics and critical exponents at and away from  $x_c$

System	$x_c(L)$	$P$ at $x_c(L)$	$\tau$	$\beta$	$\gamma$ (above $x_c$ )	$\gamma$ (below $x_c$ )
Universal value <sup>a</sup>	— <sup>b</sup>	— <sup>b</sup>	2.18	0.41	1.80	1.80
1 <sup>c</sup>	0.0969	0.0330	2.25	0.36	1.99	2.12
2a	0.0965	0.0337	2.27	0.36	1.99	2.25
2b	0.1049	0.0403	2.31	0.36	2.06	—

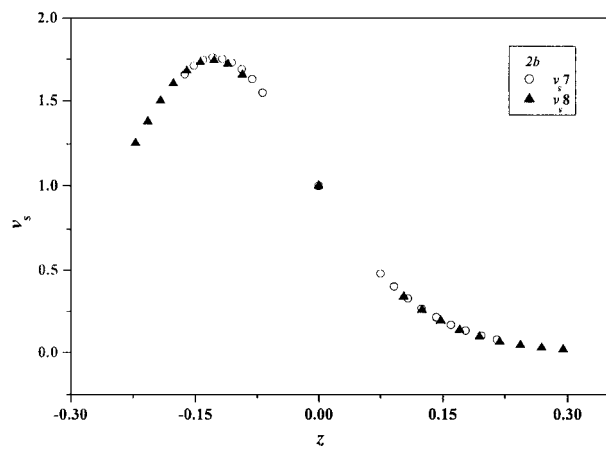
<sup>a</sup>After reference [5].

<sup>b</sup>These are system dependent characteristics.

<sup>c</sup>After reference [14].



(a)



(b)

Figure 4 (a) Plots of  $\nu_s (=n_s(x)/n_s(x_c))$  versus  $z$  for system 2a.  $\nu_{s7}$  for clusters with  $s = 64$  to 127 and  $\nu_{s8}$  for  $s = 128$  to 255. (b) Plots of  $\nu_s (=n_s(x)/n_s(x_c))$  versus  $z$  for system 2b.  $\nu_{s7}$  for clusters with  $s = 64$  to 127 and  $\nu_{s8}$  for  $s = 128$  to 255.

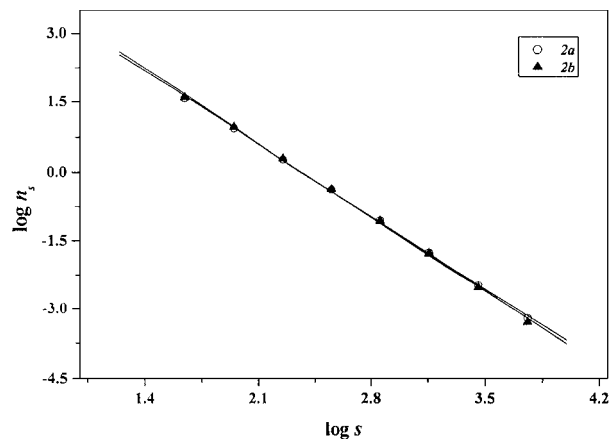


Figure 5  $\log n_s$  versus  $\log s$  plots at  $x = x_c$  for systems 2a and 2b.

The  $\beta$  values are given by the slopes of the  $\log P$  versus  $\log |x - x_c|$  plots of the considered systems (Fig. 6). The slopes for both systems 2a and 2b are same as that of system 1. The deviation from the universal value is about 10%. Fig. 7 shows  $\log S$  versus  $\log |x - x_c|$  plots when  $x_c$  is approached from above and when it is approached from below for systems 2a and 2b.

The  $\gamma$  value when  $x > x_c$  is similar for systems 1 and 2a but is slightly higher for system 2b. The deviation from the universal value is lower when  $x > x_c$  than when  $x < x_c$ . For  $x < x_c$  the deviation from the universal value

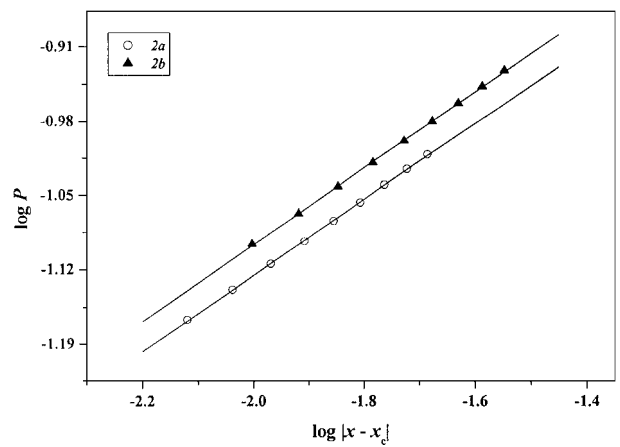


Figure 6  $\log P$  versus  $\log |x - x_c|$  for systems 2a and 2b.

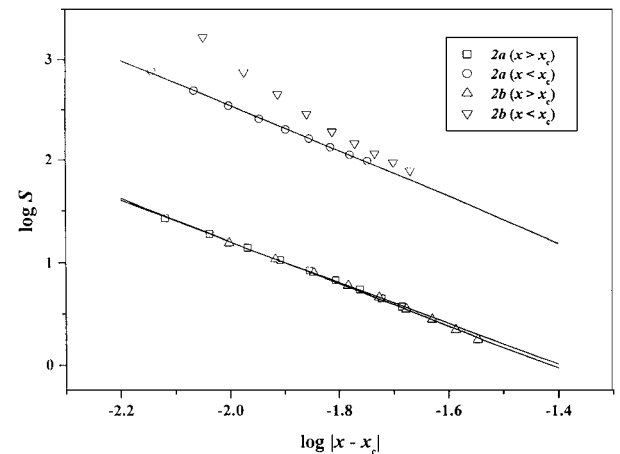


Figure 7  $\log S$  versus  $\log |x - x_c|$  for systems 2a and 2b.

is very large for system 2a. In case of system 2b, the data points show a distinctly non-linear behaviour. Hence, no linear fit has been attempted for this system and no value has been reported in Table I. However, since the scaling function has been found to be valid for all these cases therefore we may conclude that the above mentioned deviations are owing to more predominant finite size effects when  $x < x_c$ . It may be due to the formation of large clusters that are more than expected as percolation is approached.

#### 4. Conclusions

Isothermal crystallisation of glasses undergoing phase separation has been modelled using the static Monte Carlo technique as in the site percolation. Only the evolving matrix phase is assumed to have composition suitable for crystallisation at the given temperature. The experimental observations of effect of changing composition of the matrix phase on crystal nucleation and growth have been modelled in a qualitatively way. Our results suggest that due to inhomogeneous composition of the matrix during phase separation, crystal growth is impeded and consequently crystal nucleation densities may be enhanced. This may lead to finer ceramic phase microstructure in these systems than that resulting from a homogeneous glass in the initial stages of crystallisation. Further, constrained growth may affect crystal nucleation and growth leading to different induction periods for these systems.

The estimated values of the two critical exponents ( $\beta$  and  $\tau$ ) lie within acceptable deviation from their universal values but this is not the case for  $\gamma$ . The finite size effects are different for different systems and depend on their site value distributions (simulation analogue of initial compositions of systems). However, the scaling hypothesis for percolation phase transition has been found to be valid for all systems. Hence, we conclude that the universality concept has been found to be valid for all systems considered.

## References

1. P. F. JAMES, in "Glasses and Glass-Ceramics," edited by M. H. Lewis (Chapman and Hall, London, 1989) ch. 3.
2. M. TOMOZAWA, in "Treatise on Materials Science and Technology," Vol. 17 edited by M. Tomozawa and R. H. Doremus (Academic Press, London, 1979).
3. S. L. SWARTZ, A. S. BHALLA, L. E. CROSS and W. N. LAWLESS, *J. Mater. Sci.* **23** (1988) 4004.
4. W. WONG-NG, C. K. CHIANG, S. W. FRIEMAN, L. P. COOK and M. D. HILL, *Amer. Ceram. Soc. Bull.* **71** (1992) 1261.
5. D. STAUFFER and A. AHARONY, "Introduction to Percolation Theory" (Taylor and Francis, London, 1992) ch. 3.
6. A. H. RAMSDEN and P. F. JAMES, *J. Mater. Sci.* **19** (1984) 1406.
7. E. D. ZANNOTTO, P. F. JAMES and A. F. CRAIEVICH, *ibid.* **21** (1986) 3050.
8. E. D. ZANNOTTO and P. F. JAMES, in Proc. 13th Int. Glass Congress, Hamburg, Glasstech. Ber., 1983, Vol. 56K, p. 794.
9. A. BHARGAVA, J. E. SHELBY and R. L. SNYDER, *J. Non. Cryst. Solids.* **102** (1988) 136.
10. E. D. ZANNOTTO and A. GALHARDI, *ibid.* **104** (1988) 73.
11. C. W. NAN, *Progress in Materials Science* **37** (1993) 1.
12. F. YONEZAWA, S. SAKAMOTO, K. AOKI, S. NOSE and M. HORI, *J. Non. Cryst. Solids.* **106** (1988) 262.
13. K. BINDER and D. W. HEERMANN, "Monte Carlo Simulation in Statistical Physics" (Springer-Verlag, Berlin, 1988) ch. 2.
14. I. SINHA, Ph.D. thesis, BHU, Varanasi, India, 2000, ch. 3.

*Received 31 January  
and accepted 4 September 2002*